

Coincidence Spectroscopy of Highly Charged Xenon Ions by Electron Impact

M. A. Chaudhry,^(a) A. J. Duncan, R. Hippler,^(b) and H. Kleinpoppen

Atomic Physics Laboratory, University of Stirling, Stirling FK9 4LA, Scotland

(Received 10 April 1987)

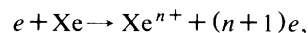
Spectroscopic studies of highly charged xenon ions (up to Xe^{9+}) produced by electron-xenon-atom collisions have been carried out in coincidence with electrons ejected at 90° to the incident electron direction and having energies between 20 and 550 eV. Relative values of partial doubly-differential ionization cross sections, $d^2\sigma^{(n)}/dE d\Omega$, for Xe^+ to Xe^{8+} have been measured for several incident electron energies between 1.0 and 8.0 keV.

PACS numbers: 34.80.Dp

There is growing interest in highly charged ions produced by inner-shell photoionization,¹ multiphoton absorption,² and charged-particle impact³ because of their importance in fields such as those of plasma physics, fusion physics, radiation physics, astrophysics, and for the production of ion sources. Ionization of many-electron atoms by electron impact is a complex phenomenon, and several processes such as direct single and double ionization,⁴ ionization-autoionization,⁵ and shakeoff⁶ are responsible for the production of various ion charge states. Multiple ionization of atoms by electron impact has been investigated³ for a long time but most of the data available refer only to total or partial ionization cross sections. Several studies⁷⁻⁹ of singly-differential cross section and doubly-differential cross section (DDCS) for ejection of secondary electrons from atomic gases by electron impact have also been reported, but

very few data exist for partial doubly-differential ionization cross sections⁷ and none for xenon atoms in the kiloelectronvolt energy range.

In this paper we report an investigation of the collision reaction,



by detection of one of the slow electrons in coincidence with xenon ions thus obtaining information about partial ionization cross sections, differential in secondary-electron energy and ejection angle.

Figure 1 shows schematically the experimental arrangement. A beam of thermal xenon atoms, emitted from a capillary array, collides with a focused beam of electrons having an energy between 1.0 and 8.0 keV. The ions produced in the interaction region are directed into a time-of-flight (TOF)-type ion analyzer by a small

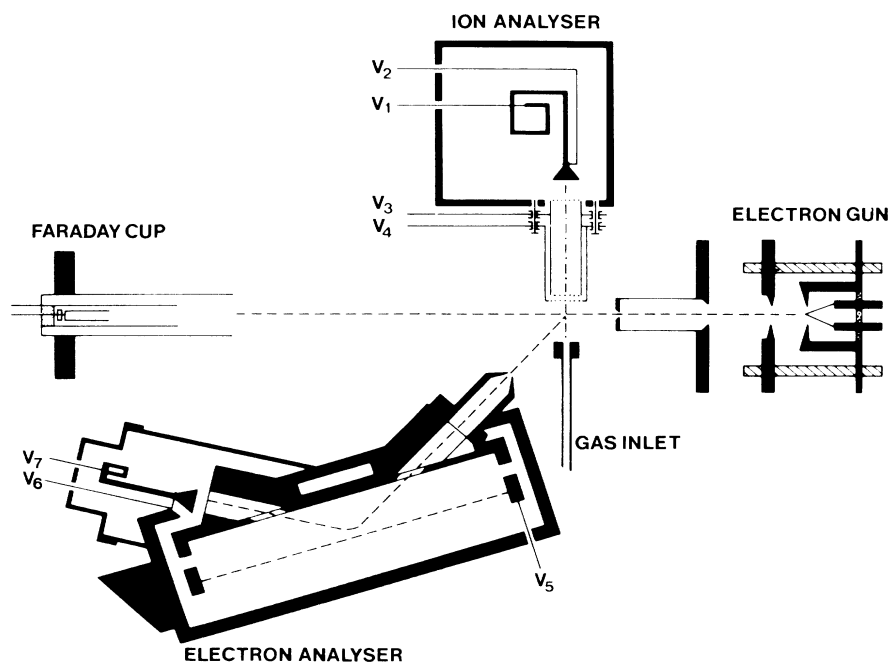


FIG. 1. Experimental arrangement for ejected-electron-ion coincidence spectroscopy.

(≈ 15 V/cm) electric field. Inside the analyzer the ions are further accelerated before drifting through a field-free region approximately 35 mm long and are detected by a Channeltron. In the diagram, V_1 and V_2 are the Channeltron voltages, while V_4 and V_3 are the extraction and drift-tube voltages, respectively, for the ion analyzer. The electrons ejected at 90° to the incident-electron direction are energy analyzed by a 30° parallel-plate electrostatic analyzer and are detected in coincidence with the product ions. The time delay of the ions relative to the ejected electrons gives information about the charge state of the ions. Figure 2 shows such a TOF spectrum for xenon ions. The incident-electron energy and the ejected-electron energy were 6.0 keV and 30 eV, respectively. Peaks for xenon ions having charges +1 to +8 can be seen clearly, while the peak for Xe^{9+} , though not much above the background, always appeared at the same position in other spectra as well.

The shape and width of the peaks are due mainly to the isotopic separation of ions of each charge state. The time spread due to the thermal velocity of the xenon atoms and the finite size of the interaction region is small in comparison.

For every charge state n , true coincidences $N_c^{(n)}$ are related to the n -fold doubly-differential cross sections, $\text{DDCS}(n+)$, by

$$\text{DDCS}(n+) = \frac{d^2\sigma^{(n)}}{dE d\Omega} = \frac{N_c^{(n)}\sigma_i}{N_i \Delta E \Delta \Omega \epsilon_\delta},$$

where σ_i is the total cross section for ion production, N_i

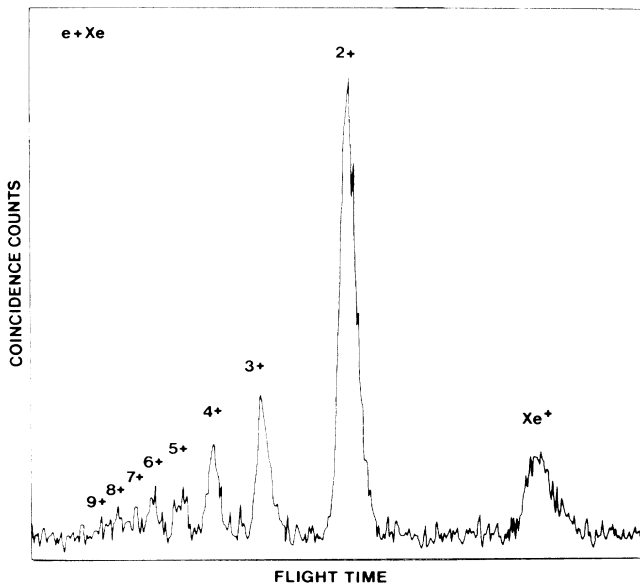


FIG. 2. Time-of-flight (TOF) spectrum of xenon ions resulting from electron impact on xenon atoms. Incident-electron energy was 6.0 keV, ejected-electron energy 30 eV, and ejection angle 90° .

is the number of detected ions, ϵ_δ is the efficiency of the electron detection system, and ΔE and $\Delta \Omega$ are the energy bandwidth and the solid angle of the electron analyzer, respectively. No attempt was made to evaluate the factor $\Delta E \Delta \Omega \epsilon_\delta$ which was, however, kept constant throughout the experiment. To keep ϵ_δ constant, potentials at the ends of the electron-analyzer Channeltron were adjusted to give the electrons incident on it a 200-eV energy, for maximum detection efficiency. For the total ionization cross section σ_i , we used the values of Schram, Boerboom, and Kistenmaker.³ The results also allowed the calculation of the mean charge $\bar{n}(E)$ of the

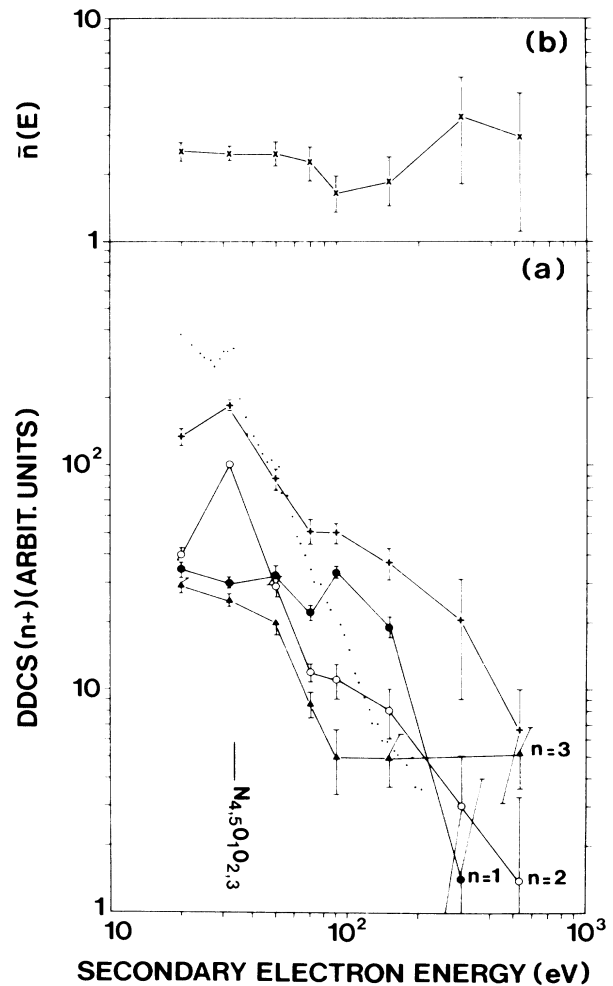


FIG. 3. (a) Relative values of the partial doubly-differential cross sections [$\text{DDCS}(n+)$] for Xe^+ (filled circles), Xe^{2+} (open circles), and Xe^{3+} (filled triangles) plotted against ejected- (secondary-) electron energy E . Incident-electron energy was 6.0 keV and ejection angle was 90° . DDCS values are marked as pluses. Lines are to guide the eye. The dotted line shows the results of Opal *et al.* (Ref. 9) for DDCS at 500-eV incident-electron energy normalized to our data at 50 eV, secondary-electron energy. (b) Mean charge $\bar{n}(E)$. Lines are to guide the eye.

ions detected in coincidence with secondary electrons having energy E , according to

$$\bar{n}(E) = \sum_n (N_c^{(n)} n) / \sum_n N_c^{(n)}.$$

Figure 3(a) shows relative values of $\text{DDCS}(n+)$ for $n=1$ to 3 and $\text{DDCS} = \sum_n \text{DDCS}(n+)$ (Nagy, Skultartz, and Schmidt³) plotted against ejected-electron energy. The DDCS generally exhibits a smooth decrease⁸⁻¹⁰ with increase in the energy of the emitted electrons. Electrons ejected from autoionization states have definite sharp energies and the corresponding spectrum is superimposed⁸ over the continuous part of the energy spectrum due to direct ionization and double Auger¹¹ transitions such as $N_{45}OOO$ which accounts for 27% of the total radiationless transition rate¹² from N_{45} subshells. The sharp increase in the DDCS corresponds to the Auger transition $N_{45}O_1O_{23}$ emitting 32.8-eV elec-

trons. Figure 3(a) also shows that our results for DDCS agree generally with similar results of Opal, Beaty, and Peterson⁹ for 500-eV incident-electron energy. However, at secondary-electron energies greater than 100 eV, our values for DDCS are higher than those of Opal, Beaty, and Peterson.⁹ This increase could be due to the several additional single¹³ and double¹¹ Auger transitions which are possible at 6.0-keV incident-electron energy.

Figure 3(b) shows the mean charge $\bar{n}(E)$ as a function of the secondary-electron energy E . The apparent decrease in the value of $\bar{n}(E)$ around 100-eV secondary-electron energy is, perhaps, due to the absence of the effect of the strong Auger transitions, such as $N_{45}O_1O_{23}$, in the region from 20 to 50 eV.

Figure 4(a) shows relative values of $\text{DDCS}(n+)$ for $n=1$ to 8 plotted against incident-electron energy for an ejected-electron energy of 30 eV and an ejection angle of 90°. Higher-order ionization is mainly produced by the removal of inner-shell electrons followed by a vacancy cascade, but, for multiple ionization to be detected in our experiment, the vacancy cascade must end at N_{45} subshells or should otherwise eject an electron of 30 eV by some other process. A vacancy in the L_i subshell, for example, has a 52.4% probability^{14,15} of being transferred to the L_{23} subshells by a Coster-Kronig transition which could be followed by several Auger transitions,¹³ such as $L_3M_3M_3$, $M_3M_5O_{45}$, $M_5N_{45}N_{45}$, and $N_{45}O_1O_{23}$, resulting in the ejection of up to five electrons. If one adds to this the contributions due to shakeoff⁶ processes as well, the high state of ionization reached in these processes is quite understandable. Figure 4(a) also shows that, at incident-electron energies higher than M -shell ionization potentials, $\text{DDCS}(n+)$ for all charges show an increase in their values. $\text{DDCS}(2+)$ and $\text{DDCS}(4+)$ have peaks at 4.0 keV, while $\text{DDCS}(3+)$ has a peak at 3.0-keV incident-electron energy. $\text{DDCS}(2+)$, $\text{DDCS}(3+)$, and $\text{DDCS}(4+)$ show jumps in their values at the L -subshell edges. A trend towards production of ions with higher charges, beyond 7.0-keV incident-electron energy, is also evident. This observation agrees generally with the results of photoionization studies^{1,16} showing that vacancies in the L shell can result in higher average charge per ion than vacancies in the M shell or N shell.

Figure 4(b) gives the variation of $\bar{n}(E)$, for $E=30$ eV, with incident-electron energy and shows evidence for a slow increase in the production of ions with higher charges as the electron energy increases above 1.0 keV. There is, however, given the size of the error, no clear indication of any steps in the quantity $\bar{n}(E)$ which might be expected just above the L -subshell edges.

In conclusion it should be noted that, while single and double ionization of atoms by electron impact is fairly well understood,¹⁷ this is not so for the process of multiple ionization. Since, in general, doubly-differential

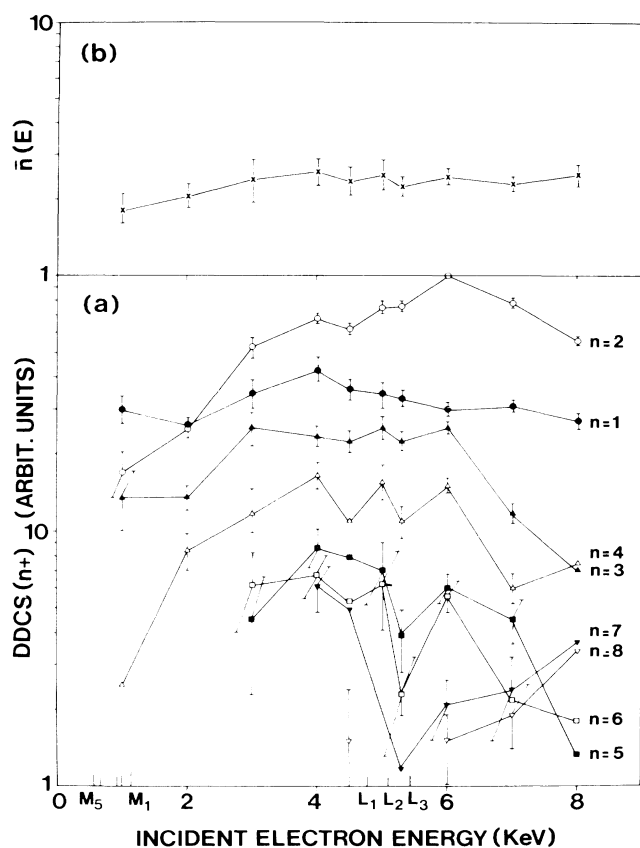


FIG. 4. (a) Relative values of the partial doubly-differential cross sections [$\text{DDCS}(n+)$] for Xe^+ (filled circles), Xe^{2+} (open circles), Xe^{3+} (filled triangles), Xe^{4+} (open triangles), Xe^{5+} (filled squares), Xe^{6+} (open squares), Xe^{7+} (filled inverted triangles), and Xe^{8+} (open inverted triangles) plotted against incident-electron energy. The ejected-electron energy was 30 eV, and the ejection angle was 90°. Lines are to guide the eye. (b) Mean charge $\bar{n}(E)$, for $E=30$ eV. Lines are to guide the eye.

cross-section measurements are much more sensitive to theoretical details than total or singly-differential cross sections, the data presented here for partial DDCCS can provide an much more critical test for mathematical models of ionization by electrons.

^(a)On leave from High Tension and Nuclear Research Laboratory, Government College, Lahore, Pakistan.

^(b)Permanent address: Fakultät für Physik, Universität Bielefeld, D4800 Bielefeld, Federal Republic of Germany.

¹R. T. Short, C.-S. O, J. C. Levin, I. A. Sellin, L. Liljiby, S. Huld, S.-E. Johansson, E. Nilsson, and D. A. Church, *Phys. Rev. Lett.* **56**, 2614–2617 (1986).

²G. Mainfray, *J. Phys. (Paris), Colloq.* **46**, 113–125 (1985); T. S. Luk, H. Plummer, K. Boyer, M. Shahidi, H. Eggar, and C. K. Rhodes, *Phys. Rev. Lett.* **51**, 110–113 (1983).

³B. L. Schram, A. J. H. Boerboom, and J. Kistemaker, *Physica (Utrecht)* **32**, 185–196 (1966); B. L. Schram, *Physica (Utrecht)* **32**, 197–208 (1966); P. Nagy, A. Skultartz, and V. Schmidt, *J. Phys. B* **13**, 1249–1267 (1980).

⁴F. D. Daniel, *Nucl. Instrum. Methods* **214**, 57–63 (1983); A. Kumar and B. N. Roy, *Can. J. Phys.* **56**, 1255–1260 (1978).

⁵A. M. Howald, D. C. Gregory, R. A. Phaneuf, D. H. Crandall, and M. S. Pindzola, *Phys. Rev. Lett.* **56**, 1675–1678 (1986); A. Muller, C. Achenbach, E. Salzborn, and R. Becker,

J. Phys. B **17**, 1427–1444 (1984).

⁶T. A. Carlson and C. W. Nester, Jr., *Phys. Rev. A* **6**, 2887–1894 (1973).

⁷M. A. Chaudhry, A. J. Duncan, R. Hippler, and H. Kleinpoppen, in *Abstracts in the Proceedings of Tenth International Conference on Atomic Physics, Tokyo, Japan, 1986*, edited by H. Narumi (North-Holland, Amsterdam, 1987); R. Hippler, K. Saeed, A. J. Duncan, and H. Kleinpoppen, *Phys. Rev. A* **6**, 3328–3331 (1984).

⁸N. Oda, F. Nishimura, and S. Tahira, *J. Phys. Soc. Jpn.* **33**, 462 (1972).

⁹C. B. Opal, E. C. Beaty, and W. K. Peterson, *At. Data* **4**, 209 (1972).

¹⁰G. N. Ogurtsov, *Zh. Eksp. Teor. Fiz.* **64**, 1149 (1973) [*Sov. Phys. JETP* **37**, 584 (1973)].

¹¹W. Mehlhorn, in *Auger-Electron Spectroscopy of Core Levels of Atoms in Atomic Inner-Shell Physics*, edited by B. Craseman (Plenum, New York, 1985), p. 121.

¹²R. B. Cairns, H. Harrison, and R. I. Schoen, *Phys. Rev.* **183**, 52 (1969).

¹³W. A. Coglean and R. E. Clansing, *At. Data* **5**, 317–469 (1973).

¹⁴R. Hippler, I. McGregor, M. Aydinol, and H. Kleinpoppen, *Phys. Rev. A* **23**, 1730–1736 (1981).

¹⁵M. H. Chen, B. Craseman, and H. Mark, *Phys. Rev. A* **24**, 177 (1981).

¹⁶T. A. Carlson, W. E. Hunt, and M. O. Krause, *Phys. Rev.* **151**, 41 (1966).

¹⁷J. H. McGuire, *Phys. Rev. Lett.* **49**, 1153–1157 (1982).